

A. Hernández-Melían^{a,*}, B. M. Huddart^a, F. L. Pratt^b, S. J. Blundell^c, M. Mills^d, H. K. S. Young^d, K. E. Preuss^d and T. Lancaster^a^aDepartment of Physics, Centre for Materials Physics, Durham University, South Road, Durham, DH1 3LE, United Kingdom^bISIS Neutron and Muon Source, STFC-RAL, Chilton, Didcot, OX11 0QX, United Kingdom^cOxford University, Clarendon Laboratory, Parks Road, Oxford, OX1 3PU, United Kingdom^dDepartment of Chemistry, University of Guelph, 50 Stone Road East, Guelph, N1G 2W1, Ontario, Canada

ARTICLE INFO

Keywords:

Muon-spin relaxation
Molecule-based magnetism
Hysteresis
Muon site determination
Density functional theory

ABSTRACT

We present the results of a muon-spin relaxation (μ^+ SR) investigation of the crystalline organic radical compound 4-(2-benzimidazolyl)-1,2,3,5-dithiadiazolyl (HbimDTDA), in which we demonstrate the hysteretic magnetic switching of the system that takes place at $T = (274 \pm 11)$ K caused by a structural phase transition. Muon-site analysis using electronic structure calculations suggests a range of candidate muon stopping sites. The sites are numerous and similar in energy but, significantly, differ between the two structural phases of the material. Despite the difference in the sites, the muon remains a faithful probe of the transition, revealing a dynamically-fluctuating magnetically disordered state in the low-temperature structural phase. In contrast, in the high temperature phase the relaxation is caused by static nuclear moments, with rapid electronic dynamics being motionally narrowed from the muon spectra.

1. Introduction

Understanding the link between hysteresis and structure is an important theme in materials design, since systems that exhibit hysteretic effects intrinsically possess memory and are therefore of potential technological interest. Recently, a crystalline organic radical compound 4-(2-benzimidazolyl)-1,2,3,5-dithiadiazolyl (HbimDTDA) was reported [1] that exhibits bistability in its magnetic and structural properties near room temperature. In the solid state, the neutral radical HbimDTDA crystallizes in an orthorhombic $Pbca$ space group (see Fig. 1). The magnetic switching effect follows from a subtle single-crystal-to-single-crystal structural phase transition centred at $T \approx 270$ K that occurs without symmetry breaking, but involves a significant reorganisation of supramolecular contacts. Structural analysis at $T = 100$ K shows that the low-temperature structure of the material involves one-dimensional linear arrays of HbimDTDA molecules, with each molecule forming part of a pancake-bonded pair with a partner molecule on a neighbouring array [Fig. 1a]. The geometry of the pancake bonds, determined by overlap of the four lobes of each molecule's singly-occupied molecular orbital, orients the molecules to create a dense 3D network of supramolecular contacts. In contrast, the high-temperature structure of the system determined at $T = 340$ K does not feature the pancake bonds, which are broken and replaced with new electrostatic contacts [Fig. 1b]. These two structural phases are related by a translation in the [010] direction, such that the one-dimensional supramolecular structures (defined by hydrogen bonding between neighbouring molecules) shift with respect to one another. Analysis of the temperature dependence of the structural phase transition confirms a

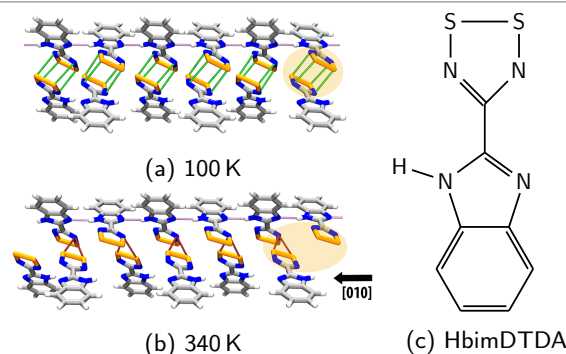


Figure 1: (a) Low-temperature structure of HbimDTDA, with pancake bonds between the linear arrays of molecules arranged along [010]. (b) High-temperature structure following a shift along [010] that breaks the pancake bonds. (c) Chemical structure diagram of single HbimDTDA molecule.

first-order transition between two unique phases, occurring around $T \approx 270$ K, with significant thermal hysteresis [1].

Each radical unit carries a $S = 1/2$ spin and the magnetism of the system is closely linked to the structural transition. Magnetic susceptibility data were reported to indicate diamagnetic low-temperature behaviour, which was explained by the electronic overlaps promoted by the pancake bonds between π -radicals. At high temperature the susceptibility increases dramatically, consistent with the non-pancake bonded phase being paramagnetic and comprising an unpaired $S = 1/2$ spin per molecule, with some degree of antiferromagnetic coupling between them. Particularly notable is the hysteretic magnetic transition between the states [1].

Implanted muons are widely used as local probes of magnetism [2], with their extreme sensitivity motivating their use to determine the magnetic order and dynamics in low-moment, molecule-based magnets. Muons have been

*Corresponding author

 alberto.hernandez-melian@durham.ac.uk (A. Hernández-Melían)
ORCID(s):

used rather less to look at magnetic bistability, though they have proved an effective probe of molecular spin-crossover (SCO) materials formed from bistable molecules that are able to switch from low to high spin states via a cooperative phase transformation [3]. In this paper we report the use of muon-spin relaxation (μ^+ SR) techniques to examine the cooperative magnetic switching in HbimDTDA from a local perspective. We show that muons are sensitive to the bistability of the magnetic state and use this to elucidate the nature of the low- and high-temperature regimes, and provide a determination of the characteristic field fluctuation rate in the low-temperature regime. We also determine the muon sites using first-principles electronic structure methods to demonstrate how the muon is sensitive to the magnetic environment in this chemically-complex material.

2. Experimental

In a μ^+ SR experiment positive muons are implanted in the sample, usually settling at interstitial sites, but quickly decay with a mean lifetime of 2.2 μ s. The muon spin polarisation, whose time-dependence is determined by the local field distribution, can be measured by studying the statistics of the positron emission in the decay, since the positron is emitted preferentially along the direction of the muon spin. The detectors around the sample are classified into forward (F) and backward (B) banks with respect to the initial muon polarisation, so that the quantity of interest, proportional to the muon spin polarisation, is the positron asymmetry function

$$A(t) = \frac{N_F(t) - \alpha N_B(t)}{N_F(t) + \alpha N_B(t)}, \quad (1)$$

where $N_F(t)$ and $N_B(t)$ are sums of the counts in all the forward and backward detectors respectively, while α is a calibration constant which accounts for the different efficiencies and geometries of the detectors and can be determined from experimental data.

To investigate the hysteresis effect and the magnetism of the two phases of the compound, μ^+ SR measurements were performed using the HiFi spectrometer at the STFC-ISIS Facility (Rutherford Appleton Laboratory, UK). We employed the longitudinal field (LF) geometry where an external magnetic field is applied along the initial muon-spin direction. Initially, a series of measurement were made in zero applied magnetic field, sweeping temperatures such that each measurement was made at a fixed temperature for 35 min, with temperature changes taking 7 min. Measurements were also made as a function of applied field at fixed temperature, for 40 min per point. We also performed weak transverse field (wTF) measurements, where a small magnetic field (2 mT) is applied perpendicular to the initial muon-spin direction. Each measurement took 24 min, with 7 min for temperature adjustment. A polycrystalline sample of HbimDTDA was prepared as described previously [1]. For the measurement it was wrapped in Ag foil, sealed in an airtight Cu holder and then loaded into a ^4He cryostat.

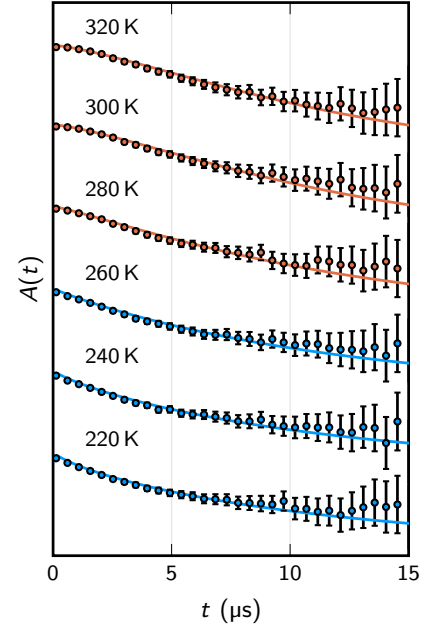


Figure 2: ZF asymmetry spectra measured on HbimDTDA at increasing temperatures across the transition, offset for clarity and therefore in arbitrary units.

3. Results

3.1. Zero-field measurements

The sample was first cooled to $T = 220$ K and a series of measurements in zero-applied field (ZF) were made in intervals of 10 K up to 350 K. Measurements were then repeated for decreasing temperature. Example spectra for measurements taken on increasing temperature are shown in Fig. 2. The observed trend is that spectra resemble an exponential relaxation at low temperatures and become more Gaussian in character as the temperature increases. To track their evolution, the spectra were fitted to a stretched exponential relaxation function

$$A(t) = A_R^{\text{ZF}} \exp\left[-(\lambda^{\text{ZF}} t)^\beta\right] + A_B^{\text{ZF}}, \quad (2)$$

where the final term A_B^{ZF} accounts for muon spins that do not relax, including those from muons implanted in the sample holder. To simplify the fitting procedure we fix the parameters which vary the least in a free fit, in this case $A_B^{\text{ZF}} = 12\%$ and $\lambda^{\text{ZF}} = 0.08 \mu\text{s}^{-1}$ by taking an average. We also find that the relaxing asymmetry A_R^{ZF} increases from 15.5% to 16.6% between the low- and high-temperature phases. The parameter β allows us to interpolate between an (i) approximately exponential decay, which results from a combination of dynamically fluctuating, disordered magnetic moments in the fast fluctuation limit; and (ii) behaviour approaching Gaussian decay, which approximates the initial relaxation of the Kubo-Toyabe function, which results from static magnetic moments sampled from a normal distribution [2].

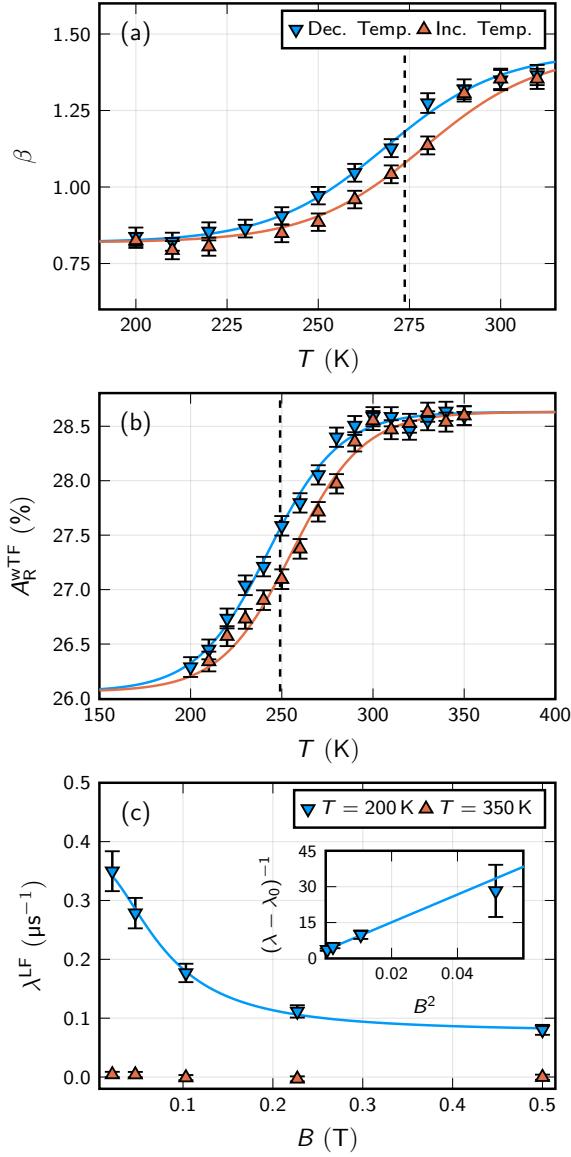


Figure 3: (a) The result of fitting a stretched exponential function [Eq. (2)] to the ZF results, showing the temperature dependence of the line-shape parameter β for increasing (Inc.) and decreasing (Dec.) temperature. (b) The result of fitting an exponentially decaying cosine curve [Eq. (4)] to the wTF results, for which we show the relaxing asymmetry A_R^{wTF} . (c) The result of fitting an exponential decay [Eq. (5)] to the field-dependent LF data, giving the relaxation parameter λ^{LF} fitted to the Redfield formula [Eq. (6)].

The results of the fitting procedure are shown in Fig. 3, where the fitted stretching parameter is seen to change as a function of temperature across a transition region [Fig. 3(a)]. We can clearly see the hysteresis effect with the decreasing-temperature measurements (down triangles) consistently at higher values than the increasing-temperature ones (up triangles) over a region centred on $T = (274 \pm 11)$ K. This value was extracted from the fitted values of β by fitting both sets

of measurements to the phenomenological functional form

$$A_R^{\text{wTF}}(T) = A_H \tanh[k_H(T - T_0)] + c_H, \quad (3)$$

where A_H , k_H and c_H are parameters which determine the shape and position of each curve and are kept constant between them whilst T_0 determines the centre and is different between the increasing and decreasing temperature curves. We can therefore determine an approximate value for the width of transition by taking the difference between the T_0 values.

The difference between the two regimes can be explained by the different distributions of fluctuating magnetic moments in each. In the low temperature phase we have randomly-oriented electronic moments (in a distribution of width $\Delta/\gamma_\mu = \sqrt{\langle B^2 \rangle}$, where $\gamma_\mu = 2\pi \times 135.5 \text{ MHz T}^{-1}$ is the muon gyromagnetic ratio) fluctuating at rate ν in the fast fluctuation limit $\nu \gg \Delta$. As the temperature increases through the transition, the density of moments increases due to the structural transition. Crucially, these moments fluctuate at a much faster rate in the higher temperature phase, with the result that the muon spin, whose evolution is limited by the value of its gyromagnetic ratio, cannot complete a rotation before the local field fluctuates and changes value [2]. The electronic moments are therefore motionally narrowed from the spectra in the high- T regime. This leaves only the random nuclear moments to account for a large part of the relaxation. The nuclear spins are quasistatic and so are described by a Kubo-Toyabe-like function (of which we only observe the early-time, Gaussian part). The fact that the value of β appears to plateau below $\beta \approx 1.5$ suggests that the motional narrowing is not complete.

3.2. Weak transverse-field measurements

In order to confirm the existence of the hysteresis loop, the temperature-dependent measurements were also repeated over the same range but in a weak transverse magnetic field ($B = 2 \text{ mT}$). Since the external field is so low, the only muon spins that will oscillate are those in sites where the local field almost vanishes in zero field, and which are not rapidly relaxed by dynamics. The size of the change we observe in amplitude with temperature is small, suggesting that those muons contributing to this effect constitute only a small fraction of the total ensemble, which might be explained by the change in the nature of the muon sites with structural phase, as discussed below. The results were fitted to a decaying sinusoidal curve

$$A(t) = A_R^{\text{wTF}} \exp(-\lambda^{\text{wTF}} t) \cos(\omega t + \phi) + A_B^{\text{wTF}}, \quad (4)$$

with the resulting relaxation asymmetry shown in Fig. 3(b). We again see a consistent separation between the measurements made in increasing and decreasing temperature over the transition region, but compared to those above, the fitted parameters have a much lower uncertainty (in part because fitting a periodic cosine wave has less margin of error than an exponential), and so the hysteresis loop is clearer. Repeating the fitting procedure used in the previous section,

we find that the loop for these measurements is centred on the slightly lower temperature of $T = (249 \pm 13)$ K. The discrepancy between this and the transition derived from the change in the β parameter suggests the two measurements are sensitive to different aspects of the muon's interaction with the system: β reflects the distribution of local magnetic fields; A_R^{wTF} reflects the availability of muon sites in the two regimes, as described below. We note also that for both sets of measurements the transition appears to be continuous, although the resolution is not sufficient to rule out steps on the scale of ≈ 10 K.

3.3. Longitudinal-field measurements

To elucidate the dynamic response, a series of LF measurement were performed at both $T = 200$ K and $T = 350$ K by applying a series of external magnetic fields (up to $B = 0.5$ T) along the direction of the muon spin. As the field magnitude increases the Zeeman term in the muon's Hamiltonian dominates, and the muon spin is pinned along its initial direction. Time-varying local fields can then cause a muon spin flip and relax the asymmetry. This state of affairs allows us to investigate the magnetic-moment dynamics in the two phases by fitting the results to a series of exponential functions, quantifying the relaxation due to the fluctuating magnetic fields. This is appropriate even in the high T limit, since the applied field rapidly quenches the Gaussian relaxation, leaving residual exponential relaxation reflecting electronic dynamics. The model used is therefore

$$A(t) = A_R^{\text{LF}} \exp(-\lambda^{\text{LF}} t) + A_B^{\text{LF}}, \quad (5)$$

where we fix the parameter $A_B^{\text{LF}} = 10\%$ to simplify the fitting procedure. The value of the relaxation rate λ^{LF} is also shown in Fig. 3(c) for both temperatures. We see that only the low-temperature measurements show a decrease with increasing magnetic field. This relationship can be fitted to the Redfield formula [2]

$$\lambda^{\text{LF}} = \frac{2\Delta^2\nu}{\nu^2 + \gamma_\mu^2 B_0^2} + \lambda_0, \quad (6)$$

where Δ is the fluctuating amplitude ($\Delta^2/\gamma_\mu^2 = \langle(\delta B)^2\rangle$), ν is fluctuation rate (related to $\tau = \nu^{-1}$ the correlation time between changes), B_0 is the applied external field and λ_0 is an offset accounting for the component of the relaxation not reduced by the external field. (Such an offset is often observed in dynamically-fluctuating molecular systems [4]). This gives values of $\nu = 66(12)$ MHz and $\Delta = 3.1(3) \mu\text{s}^{-1}$ for the parameters. In the high-temperature phase a very small relaxation rate is observed in applied field, confirming that the ZF relaxation is caused by static nuclear moments, which are unable to cause the required spin flips. On the other hand, the successful description of the low-temperature relaxation parameters with the Redfield formula confirms that the muon-spin relaxation is caused by randomized electronic moments with dynamics in the fast-fluctuation limit.

4. Muon site analysis

First-principles calculations allow us to compute candidate muon sites and gain an insight into how the muon probes materials. This method (DFT+ μ [5–7]) involves performing a geometry optimisation calculation of the structure with an additional reduced-mass hydrogen atom representing a bare muon (Mu^+) or a muonium (Mu^0) atom. The initial implantation site is chosen randomly with the constraint that initial positions must be a minimum distance of 1 \AA from the atoms and 0.5 \AA from the other sites. The simulations were run on a $8.6 \times 9.9 \times 21.4 \text{ \AA}$ unit cell of the crystal structure of HbimDTDA using the CASTEP code [8] with files generated by the MuFinder program [6], producing 30 candidate sites for each phase. The relaxed unit cells were analysed first by considering the distortions to the atomic positions caused by the muon, which in this case are minimal between atoms of the same molecule but more considerable between molecules, with a maximum radial displacement of $\sim 1.0 \text{ \AA}$, especially for the sites $\bar{\text{H}}$ / ■ and H / ■ described below. Muon sites corresponding to different relaxed structures were compared by using the vector between the site and closest atom to position the muons in a undistorted cell. Finally the symmetry of the crystal was used to move all the sites to the same molecule and nearby sites ($d < 1 \text{ \AA}$) were grouped together by averaging their positions. All the muonium site simulations were also repeated for a bare muon, by not adding an extra electron to the system for the muon. This gave similar results, so that sites were matched with the muonium ones by assuming that ones closer than 0.5 \AA are equivalent. All sites were realised in both cases with the exception of a single muon site (denoted S_1 / ■ below) which was not found in the high-temperature phase (details can be found in the Supplemental Material [9]).

The positions of the calculated candidate muon sites are shown in Fig. 4 (only for the case of Mu^0 but the others are similar) and their respective energies are listed in Table 1. Energies are given relative to the lowest-energy site for each column. The similarity in energy between the candidate sites in each class suggests that we might expect each of them to be realised. We first find a set of candidate sites common to both structures close to the nitrogen atoms in the sulphur-containing rings. Two of them (S_1 / ■ and S_2 / ■) are located *outside* the region between rings in adjacent chains (see shaded area in Fig. 1a), with the second being *closer* to the atoms which form the contact bond between chains in the high temperature phase (see Fig. 1b). Another site (S_3 / ■) is located *inside* the region but *away* from the contact sulphur atoms, which might explain why it has a similar energy at the lower temperature but is higher in energy at 340 K. The other low-temperature site ($\bar{\text{H}}$ / ■) has the muon attached to the non-hydrogenated nitrogen atom in the central ring and is higher in energy for muonium but the lowest energy site in the case of the bare muon.

Apart from these common sites, for the 340 K structure we also find two new lower-energy sites. One (H / ■) is found sharing the nitrogen atom with a hydrogen atom in the central ring (see Fig. 1c) and the other (S_4 / ■) is

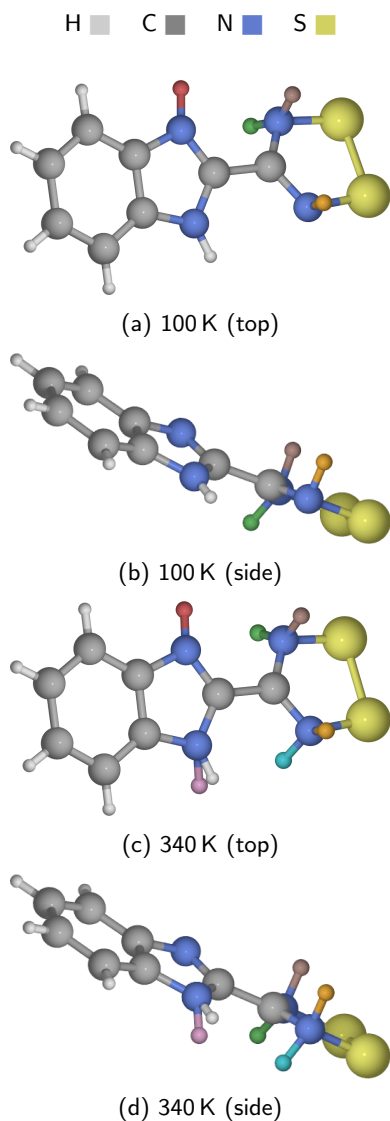


Figure 4: Diagrams showing the main sites for muonium at (a,b) 100 K, with three low-energy sites (orange, green and brown) and a slightly higher-energy site (red) (c,d) 340 K, with two new lower energy sites (pink and cyan)

again attached to one of the nitrogen atoms in the sulphur-containing ring, but in this case is *inside* the inter-ring region and *closer* to the contact atoms. To explain the presence of the new sites we note that the main difference between the two structural phases is the presence of the pancake bonds between the sulphur rings in the lower-temperature state and the relative position of the chain. The breaking of these bonds at higher temperature seems to make the new positions available.

5. Discussion

Conventionally we assume that a bare (or diamagnetic) muon spin couples to the local magnetic field in a material, and probes the local field distribution without causing an appreciable perturbation. The relevant muon sites from the

Site	Energy (eV)			
	Mu ⁰		Mu ⁺	
	100 K	340 K	100 K	340 K
S ₁ (orange)	0.01	0.06	0.43	-
S ₂ (green)	0.01	0.17	0.38	0.93
S ₃ (red)	0.12	0.14	0.00	0.00
H̄ (brown)	0.00	0.06	0.37	0.24
H (pink)	-	0.05	-	0.00
S ₄ (cyan)	-	0.00	-	0.23

Table 1

Table comparing the energies of the unit cell with the muon at the different bare muon (Mu⁺) and muonium (Mu⁰) sites calculated using DFT, and given relative to the lowest energy found in each column.

previous section would then be the bare ones. The low-temperature regime of this material, which is thought to be formed from singlet spins, was previously suggested to be diamagnetic on the basis of bulk susceptibility measurements. However, if the muon takes the form of an unperturbing, diamagnetic probe, then the low-temperature relaxation cannot simply be explained by the presence of highly-dilute magnetic impurities in a diamagnetic background, since the Redfield behaviour observed relies on the presence of a dense array of magnetic moments that rapidly fluctuate in time. It might therefore be unlikely that the material can be characterised as being non-magnetic in this regime, but rather there are fluctuating moments of sufficient density to be approximated as giving rise to a Gaussian distribution of fields at any instant. We distinguish the local magnetic field distribution in the low temperature phase, featuring this distribution of moments fluctuating in the fast fluctuation limit, from that in the high-temperature regime, which likely comprises a denser distribution of moments, with a far greater characteristic fluctuation rate.

Since the muon is a local probe, the transition we observe likely reflects muons locally detecting the switching of nearby clusters of molecules in the sample. A cluster in the low-temperature state giving an exponential relaxation and one in the high-temperature state a Gaussian one. The stretched exponential used in the intermediate regime then models the sum of contributions, whose relative size varies with temperature. We note that our results in this system resemble those measured in spin-crossover systems based on iron (II) ions which show a crossover between a low-spin ($S = 0$) state at low temperature and a high-spin ($S = 2$) state at high temperature [3, 10]. In those materials the muon spectra were also fitted to a stretched-exponential function with $\beta < 1$ in the low temperature, low-spin configuration and β approaching $\beta = 2$ at high temperature. It was suggested that the relaxation at low temperature reflected an incomplete crossover, with some spins remaining in the high-spin configuration at low temperature and forming a very dilute distribution leading to root-exponential relaxation [11]. A similar picture could be the case here, with any

regions that avoid the low-temperature structural transition giving rise to a distribution of disordered spins, causing the observed relaxation. However, the fact that we find $\beta \lesssim 1$ suggests that the density of moments in our system at low temperature is greater than the highly-dilute one that would be expected to give rise to $\beta \approx 0.5$, which was the value observed in some of the low-temperature phases of the iron-based spin-crossover systems [10].

Another possibility which could account for our data is that the muon's sensitivity to the magnetism in the low-temperature, singlet state is caused by a perturbation the muon makes to the system, as was suggested to be the case in molecular spin-ladder materials [5]. This might involve the bare, charged muon causing a local distortion to the nearest spin singlet, or that the sensitive species is derived from muonium, whose extra electron is involved in causing the necessary distortion. The muon, along with its local distortion, would then become the sensitive species, whose interactions give rise to the observed relaxation. We note that the observed fluctuation amplitude Δ in this regime corresponds to the magnetic field from an electron spin around $\approx 6 \text{ \AA}$ from a muon, providing a rough length scale for the interaction. If this is the case, then the material could adopt a fairly uniform singlet ground state with few additional intrinsic magnetic impurities. However, even in this case, the transition to a regime of large, dense magnetic moments at high temperature would continue to allow the muon to faithfully probe the magnetic switching transition.

Finally, the difference in the low-energy muon sites in this material's two structural phases is a noteworthy feature, as the difference in sites in different states of a system has not been discussed previously in materials of this type. Since we find a range of muon sites in this system with very similar energy, we would expect the muons to sample a range of internal magnetic fields. Although both a bare muon and muonium allow several different low-energy candidate sites in the two temperature regimes, owing to the range of fields probed, the two cases are unlikely to lead to cause significant differences in to the measured spectra. However, the observation of new sites becoming available after a structural change likely applies well beyond this material.

Important questions remain about the nature of the phase transition in this system, particularly related to the broadness of the transition compared to the width of the hysteretic region. Inspection of the magnetic susceptibility data suggests the presence of steps in the response. Indeed, tracking the structural component of the transition as a function of T by powder x-ray diffraction also suggests a stepwise progression, with reflections consistent with the high temperature phase appearing over a range of temperatures. There has been recent interest in the possibility of realizing the devil's staircase structure in such systems [12], where step-like transitions between the spin states have been observed.

6. Conclusion

Muon-spin relaxation measurements, paired with muon-site analysis, have allowed us to probe the hysteretic magnetic switching behaviour of HbimDTDA from a local perspective. We identify a hysteresis width of $\Delta T \approx 22 \text{ K}$, centred on $T = 274 \text{ K}$. The low-temperature state gives rise to muon-spin relaxation which is well described by a model that assumes a dense arrangement of disordered, dynamically-fluctuating moments. The structural transition causes the muon sites in the two regimes to differ. However, in a chemically-complex material such as this, a large number of sites of similar energy occur in both regimes, with the result that we expect the muon to faithfully probe the system across the transition. Although this latter feature of differing muon sites in different structural regimes has yet to be widely investigated, it is possible that it is a general feature that we should expect in numerous systems.

7. Acknowledgments

Part of this work was performed at the STFC-ISIS facility and we are grateful for provision of beamtime and access to the SCARF Computer cluster. We are also grateful for computational support provided by both Durham Hamilton HPC and by the UK national high performance computing service, ARCHER2, for which access was obtained via the UKCP consortium and funded by EPSRC. AHM is grateful to STFC and EPSRC for the provision of a studentship. For the purpose of open access, the authors has applied a Creative Commons Attribution (CC BY) licence to any Author Accepted Manuscript version arising. Research data from this project will be made available via Durham Collections.

References

- [1] Mills M B, Wohlhauser T, Stein B, Verduyn W R, Song E, Dechambenoit P, Rouzières M, Clérac R and Preuss K E 2018 *Journal of the American Chemical Society* **140** 16904–16908 URL <http://dx.doi.org/10.1021/jacs.8b10370>
- [2] Blundell S J, De Renzi R, Lancaster T and Pratt F L (eds) *Muon Spectroscopy: An Introduction* (Oxford University Press) ISBN 978-0198858959
- [3] Blundell S J, Pratt F L, Marshall I M, Steer C A, Hayes W, Létard J F, Heath S, Caneschi A and Gatteschi D 2003 *Synthetic Metals* **133–134** 531–533 URL [http://dx.doi.org/10.1016/S0379-6779\(02\)00424-1](http://dx.doi.org/10.1016/S0379-6779(02)00424-1)
- [4] Lancaster T, Blundell S J, Pratt F L, Brooks M L, Manson J L, Brechin E K, Cadiou C, Low D, McInnes E J L and Winpenny R E P 2004 *Journal of Physics: Condensed Matter* **16** S4563–S4582 ISSN 1361-648X URL <http://dx.doi.org/10.1088/0953-8984/16/40/009>
- [5] Lancaster T, Xiao F, Huddart B M, Williams R C, Pratt F L, Blundell S J, Clark S J, Scheuermann R, Goko T, Ward S, Manson J L, Rüegg C and Krämer K W 2018 *New Journal of Physics* **20** 103002 ISSN 1367-2630 URL <http://dx.doi.org/10.1088/1367-2630/aae21a>
- [6] Huddart B M, Hernández-Melián A, Hicken T J, Gomilšek M, Hawkhead Z, Clark S J, Pratt F L and Lancaster T 2021 MuFinder: A program to determine and analyse muon stopping sites (*Preprint* 2110.07341v1)
- [7] Blundell S J, Möller J S, Lancaster T, Baker P J, Pratt F L, Seber G and Lahti P M 2013 *Physical Review B* **88** ISSN 1550-235X URL <http://dx.doi.org/10.1103/PhysRevB.88.064423>
- [8] Clark S J, Segall M D, Pickard C J, Hasnip P J, Probert M I J, Refson K and Payne M C 2005 *Zeitschrift für Kristallographie - Crystalline*

Materials **220** 567–570 URL <http://dx.doi.org/10.1524/zkri.220.5.567.65075>

- [9] See Supplemental Material for relaxed atomic structures from each of the muon site calculations.
- [10] Blundell S J, Pratt F L, Steer C A, Marshall I M and Létard J F 2004 *J. Phys. Chem. Sol.* **65** 25–28 URL <https://www.sciencedirect.com/science/article/pii/S0022369703003263>
- [11] Uemura Y J, Yamazaki T, Harshman D R, Senba M and Ansaldo E J 1985 *Phys. Rev. B* **31** 546–563 URL <https://link.aps.org/doi/10.1103/PhysRevB.31.546>
- [12] Trzop E, Zhang D, Piñeiro-Lopez L, Valverde-Muñoz F J, Carmen Muñoz M, Palatinus L, Guerin L, Cailleau H, Real J A and Collet E 2016 *Angewandte Chemie International Edition* **55** 8675–8679 URL <http://dx.doi.org/10.1002/anie.201602441>